PERGAMON

International Journal of Solids and Structures 38 (2001) 8345–8358

INTERNATIONAL JOURNAL OF SOLIDS and STRUCTURES

www.elsevier.com/locate/ijsolstr

Lifetime evaluation of cracked shaft sleeve of reactor coolant pump under thermal striping

Lih-Jier Young *

Department of Applied Mathematics, Chung-Hua University, 30 Tung-Shing, Hsin-Chu 30067, Taiwan, ROC

Received 25 July 2000; in revised form 8 May 2001

Abstract

Thermal striping of a shaft sleeve of a reactor coolant pump at a nuclear power plant is caused by incomplete mixing of the low temperature cooling water flow from water seals and high temperature cooling water flow from the reactor. Temperature fluctuation results in a significant thermal fatigue damage and therefore, a network of longitudinal cracks is found on the outer surface of sleeve. After conservative computation and evaluation by considering thermal and mechanical stresses and fracture mechanics, it was found that the crack on the surface of sleeve will become deeper according to high frequency fatigue model if the depth of the crack is larger than 10% of sleeve wall thickness. Although the sleeve will not break dramatically before one crack through the wall of sleeve they may combine with one another and cause damage to the sleeve. Therefore, in this paper the life time of the sleeve is assumed to be the time needed for one crack to propagate through the wall of the sleeve. The life assessment for the sleeve, subject to surface temperature fluctuation, is presented.

Keywords: Thermal striping; Thermal fatigue; Temperature fluctuation; Fracture mechanics

1. Introduction

Due to the incomplete mixing of low temperature cooling water flow from water seals and high temperature cooling water flow from the reactor, there is a network of cracks on the surface of the impeller shaft. The phenomenon of temperature fluctuation is called thermal striping. The character is that the changing rate of temperature will decrease from outside of the shaft and there is almost no temperature change around the core. Thermal fatigue therefore causes some damage on the shaft. Practically, a shaft sleeve is usually added to prevent thermal striping on the surface of the impeller shaft. However, several longitudinal cracks parallel to one another are found on the surface of the sleeve. There are typical thermal fatigue cracks. To ascertain whether the crack will extend deeper under normal operation is the primary purpose of this paper.

* Tel.: +886-3-537-4281; fax: +886-3-537-3771.
E-mail address: young@chu.edu.tw (L.-J. Young).

0020-7683/01/$ - see front matter
PII: S0020-7683(01)00116-0

2. Method of approach

The process of this research is as follows:

(1) The computation of stress distribution in the rotating sleeve and the analysis of shrink-fit stress in the sleeve.
(2) The distribution of periodic temperature change of the sleeve surface and the analysis on the corresponding thermal stress.
(3) The evaluation of lifetime and the analysis on the integrity of the sleeve based on fracture mechanics.

The process mentioned above should be integrated to a complete analysis model as shown in Fig. 1.

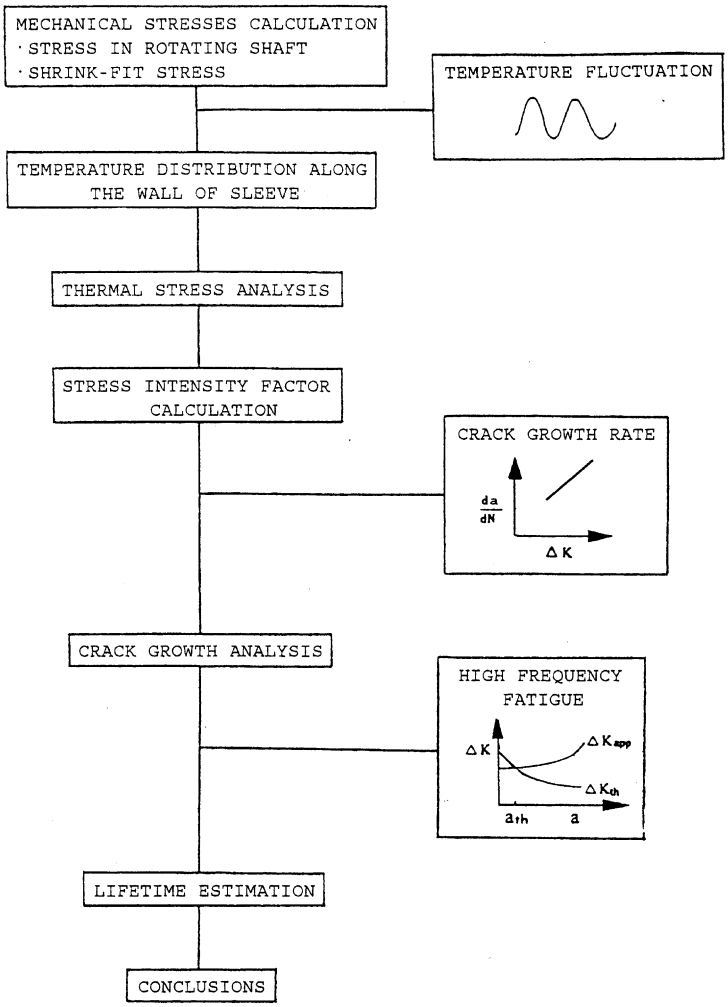

Fig. 1. Flow chart of the lifetime estimation of sleeve.

3. Stress distribution in rotating sleeve and shrink-fit stress in sleeve

During operation, the shaft and the sleeve of the reactor cooling pump are both loaded by the inertia force and steady state shrink-fit stress. In addition, they may also be loaded by unsymmetric water pressure from the impeller, radial impact and periodic vibration. These loadings may cause significant damage during operation. However, if we observe only the way of angular deflection at the contact surface between the shaft and the sleeve then

$$\theta = \frac{M_{sh}L}{EI_{sh}} = \frac{M_{sl}L}{EI_{sl}}, \tag{1}$$

where E is the Young's modulus, L is the length, θ is the angular deflection for both shaft and sleeve, M_{sh} and M_{sl} are the applied bending moments, I_{sh} and I_{sl} are moments of inertia for the shaft and sleeve, respectively. M_{sl} is much smaller than M_{sh} because I_{sl} is much smaller than I_{sh} (according to the dimensions shown in Fig. 2). Consequently, M_{sl} can be neglected during the process of stress analysis, i.e., only the stress during rotation and the shrink-fit stress need to be considered.

3.1. Stress distribution in rotating sleeve

For a rotating sleeve with angular velocity ω there are two stress components, i.e., the normal stress in the radial direction σ_r and the normal stress in the circumferential direction σ_θ. These stresses was found by Timoshenko and Goodier (1970) as

$$\sigma_r = A - \frac{B}{r^2} - \frac{3+v}{8}\rho\omega^2 r^2, \tag{2}$$

$$\sigma_\theta = A + \frac{B}{r^2} - \frac{1+3v}{8}\rho\omega^2 r^2, \tag{3}$$

where the value of ω is 1185 rpm, ρ is the mass per unit volume of sleeve (304 SS CF8 stainless steel, 0.29 lb/in.^{3}), r is the distance from the centre of the sleeve, v is the Poissons ratio (0.3) and A, B are both integration

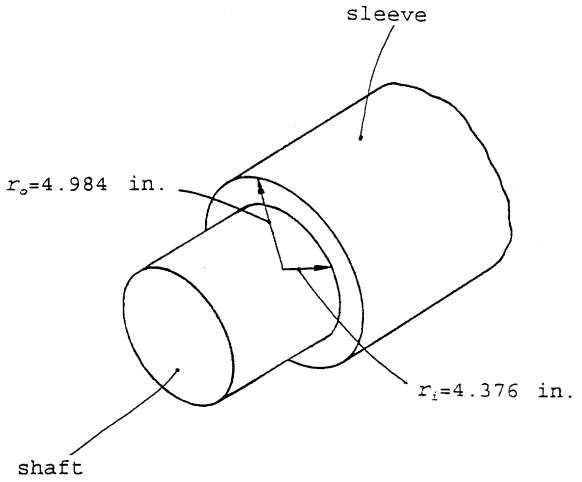

Fig. 2. Dimensions of shaft and sleeve.

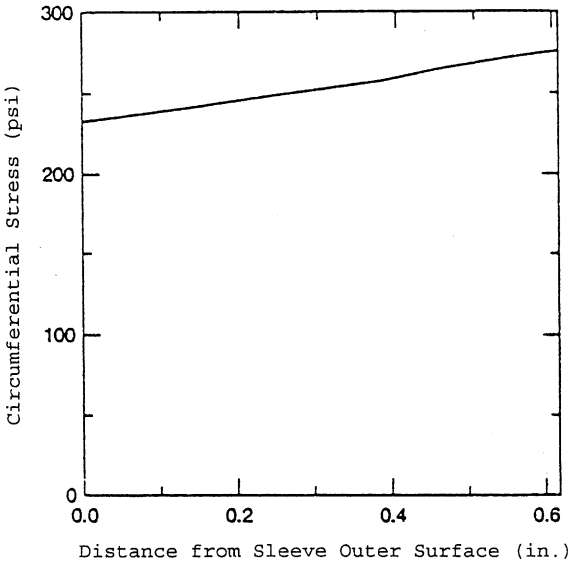

Fig. 3. Distribution of circumferential stress along sleeve wall for rotating sleeve.

constants. Since σ_r on both the inner and outer surfaces ($r = r_i = 4.376$ in. and $r = r_o = 4.984$ in.) of sleeve should be zero, the two constants A, B are found by applying these boundary conditions to Eqs. (2) and (3), i.e.,

$$A = \frac{3+v}{8}\rho\omega^2(r_i^2 + r_o^2), \tag{4}$$

$$B = \frac{3+v}{8}\rho\omega^2 r_i^2 r_o^2. \tag{5}$$

Fig. 3 shows the distribution of the circumferential stress along the wall of sleeve after substituting corresponding values of ω, ρ and v into Eqs. (4), (5) and (3). It is found that the maximum value of σ_θ is 276 psi in the inner surface ($r = r_i$) of the wall and the minimum is 233 psi in the outer surface ($r = r_o$). Although the value of σ_θ is much smaller than the shrink-fit stress calculated below it still needs to be considered to get a more conservative lifetime estimation of sleeve.

3.2. The shrink-fit stress

During the heating process both the surface of shaft and the inner surface of sleeve are under uniform compression. The magnitude of this compression depends on the difference between the outer radius (r_o) and the inner radius (r_i) of sleeve. From the Lame equation of elasticity by Timoshenko and Goodier (1970):

$$\sigma_r = C - \frac{D}{r^2}, \tag{6}$$

$$\sigma_\theta = C + \frac{D}{r^2} \tag{7}$$

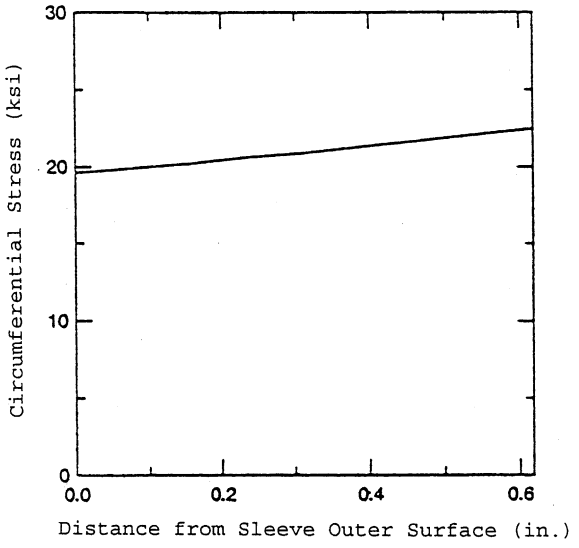

Fig. 4. Distribution of circumferential stress along sleeve wall for shrink-fit stress.

the values of circumferential and radial stress distributions can be obtained by introducing the following boundary conditions:

$$\sigma_r|_{r=r_o} = 0, \tag{8}$$

$$\varepsilon_\theta|_{r=r_o} = \frac{(\sigma_\theta|_{r=r_o} - \nu\sigma_r|_{r=r_o})}{E} = \frac{\sigma_\theta|_{r=r_o}}{E}, \tag{9}$$

where E is the Young's modulus (28000 ksi), $\varepsilon_\theta|_{r=r_o}$ is the strain of the outer surface of sleeve and usually around 0.07%. The circumferential stress on the outer surface of sleeve is therefore obtained from Eqs. (8) and (9), i.e.,

$$\sigma_\theta|_{r=r_o} = E\varepsilon_\theta|_{r=r_o} = E0.07\% = 19.6 \text{ ksi}. \tag{10}$$

From Eqs. (6)–(8) and (10) the expression of the circumferential stress σ_θ is

$$\sigma_\theta = 9.8 + \frac{243.4}{r^2}. \tag{11}$$

Fig. 4 shows distribution of the circumferential stress along the wall of sleeve. It should be clear by now that the shrink-fit stress σ_θ is too large to be neglected in the evaluation process.

4. Temperature distribution and thermal stress analysis

According to the regulation of the ASME (1989), thermal stress is a secondary stress. The effect of thermal stress on the material could be reduced by a small amount of deflection. Therefore, there will be no

damage for deductile material if thermal stress is the only loading. However, damage does occur when thermal stress is a cyclic loading or associates with another primary loading.

4.1. Temperature distribution

For a thin-wall cylinder, approximated by a plate with thickness t and temperature fluctuation of a fluid, the range of temperature change ($\Delta\theta$) of which decays exponentially from the surface according to Gruter and Huget (1982), i.e.,

$$\Delta\theta(x) = \frac{1}{\sqrt{2M^2 + 2M + 1}} \Delta T \mathrm{e}^{-\sqrt{\frac{\omega_T}{2\alpha}}x}, \tag{12}$$

where

$$M = \left(\frac{K}{h_f}\right)\sqrt{\frac{\omega_T}{2\alpha}}, \tag{13}$$

ΔT is the temperature change of the fluid, ω_T is the circular frequency of the temperature change, f (Hz) is the cyclic frequency of the temperature change ($f = \omega_T/2\pi$), α is the thermal diffusivity, x is the distance from the surface of the plate, K is the thermal conductivity, h_f is the heat-transfer coefficient. Because the ratio of the outer radius to the wall thickness of the sleeve is large enough ($r_o/t \approx 8.2$), Eq. (12) can be employed to analyse the temperature distribution along the wall thickness of the sleeve. The heat-transfer coefficient h_f in Eq. (13) of the mixed stream according to Sun et al. (1982) can be obtained as follows

$$h_f = \frac{K}{D_f}(Nu_0)\left(\frac{Nu}{Nu_0}\right), \tag{14}$$

where

$$Nu_0 = \frac{RePr\frac{C_f}{2}}{[12.7(\frac{C_f}{2})^{0.5}(Pr^{0.67} - 1) + 1.07]} \tag{15}$$

is the Nusselt number of the mixed stream at the reference point (Petukhov and Kirrilou equation), Re is the Reynolds number, Pr is the Prandtl number, C_f is the coefficient of friction,

$$Nu = Nu_0\left(\frac{1 + 4500Gr}{Re^{2.63}}Pr^{0.5}\right)^{0.31} \tag{16}$$

is the Nusselt number of the mixed stream, and Gr is the Grasnof number, D_f is the diameter of the fluid stream. The heat-transfer coefficient of Eq. (14) at different values of temperature can be simplified as a function of the velocity of the mixed stream outside sleeve as shown in Fig. 5. Finally, the value of h_f can be reached (750 Btu/h ft^2 °F) from Fig. 5 by observing that the velocity of the mixed stream is 2 ft/s (5 gpm).

Therefore, to estimate the lifetime of sleeve more conservatively, $h_f = 1000$ Btu/h ft^2 °F and $f = 1$ Hz (1–2.5 Hz usually after personal communicated with Byron Jackson water pump manufacturing company) are assumed. Other parameters which needed in Eq. (12) are $\Delta T = 460$°F (97°F temperature of water seal and 557°F temperature of reactor), $K = 9.5$ Btu/h ft °F, $\alpha = 0.16$ ft^2/h. Fig. 6 is the distribution of the range of temperature change along the wall of sleeve by using Eq. (12). It is clear that the temperature change is

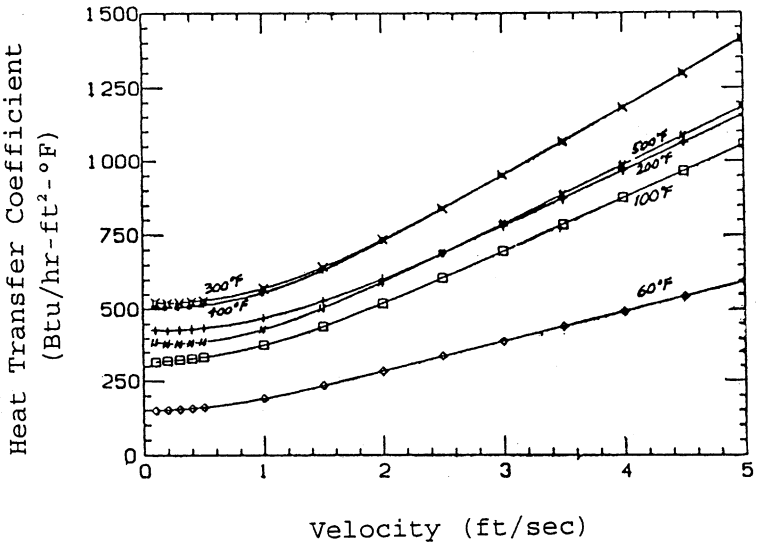

Fig. 5. Relation between velocity and heat transfer coefficient for mixed convection heat transfer.

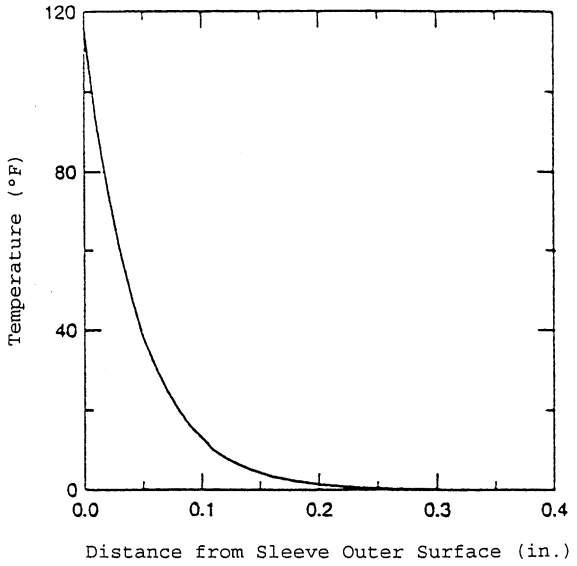

Fig. 6. Distribution of range of temperature change along sleeve wall.

very small after passing 0.2 in. (1/3rd of the thickness) from outer surface of sleeve. It means that this region is not affected by surface temperature fluctuation.

4.2. Cyclic thermal stress analysis

For a fully restrained tube with a thermal gradient in the radial direction, the cyclic thermal stress ($\Delta\sigma_{th}$) at any point is

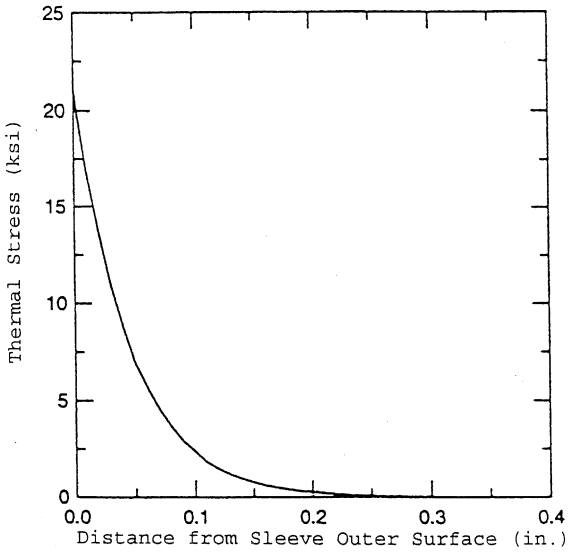

Fig. 7. Distribution of cyclic thermal stress along sleeve wall.

$$\Delta\sigma_{\text{th}} = \frac{E\alpha_{\text{t}}(\Delta\theta)}{2(1-v)}, \tag{17}$$

where E is the Young's modulus (28000 ksi), α_{t} is the thermal coefficient of expansion (9.1×10^{-6} in./in./°F), v is the Poisson's ratio and $\Delta\theta$ is the range of temperature change of any point. The substitution of Eq. (12) into Eq. (17) yields the cyclic thermal stress distribution along the wall of sleeve is shown as in Fig. 7. The maximum thermal $\Delta\sigma_{\text{th max}}$ (21.1 ksi) occurs on the outer surface of sleeve and decreases toward the inner. It seems that the distribution of thermal stress will decrease the driving force of the crack growth. The lifetime estimation of the sleeve below is more conservative because thermal stress is not taken into consideration during the stress intensity factor calculation.

5. Fracture mechanics evaluation

As mentioned above, the cracks on the surface of sleeve are longitudinal parallel cracks. The coefficient of interaction (F_{I}) between these cracks may reduce the stress intensity factors. Fig. 8 shows two parallel cracks and with crack length $2a$ of each. The distance between them is $2b$. The stress intensity factor of each crack by Jiang et al. (1991) is

$$K_{\text{I}} = F_{\text{I}}\frac{2}{\pi}\sigma\sqrt{\pi a}, \tag{18}$$

where σ is the applied normal stress. The coefficient of interaction, F_{I}, by Tada et al. (1985) is

$$F_{\text{I}} = 1 - 0.293s\left[1-(1-s)^4\right] < 1, \tag{19}$$

where $s = a/(a+b)$. Obviously, if the number of parallel cracks is more than just two the value of K_{I} will be reduced more. However, the actual value of K_{I} for a cylinder with multiple parallel cracks is not available at this moment. The value of F_{I} is therefore, assumed to be 1 (single crack) in this paper to obtain a more conservative solution.

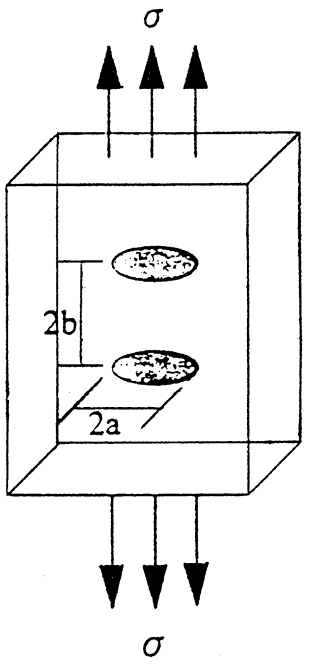

Fig. 8. Two parallel cracks within finite plate.

5.1. Stress intensity factor

For a single crack as in Fig. 9, the stress intensity factor can be expressed as in (Raju and Newman, 1982)

$$K_{\mathrm{I}} = \sqrt{\frac{\pi c}{Q}}(G_0A_0 + G_1A_1c + G_2A_2c^2 + G_3A_3c^3), \tag{20}$$

where

$$Q = 1 + 1.464\left(\frac{c}{a}\right)^{1.65} \tag{21}$$

is the coefficient of the crack shape, c is the depth of the crack, $2a$ is the length of the crack. G_0, G_1, G_2, G_3 are geometry-dependent constants.

The stress distribution perpendicular to the surface of the crack can be modelled by a polynomial of order 3.

$$\sigma(x) = A_0 + A_1x + A_2x^2 + A_3x^3, \tag{22}$$

where x is the distance from the outer surface of the sleeve, A_0, A_1, A_2, A_3 are constants. Superimposing the two circumferential stresses in Eqs. (3) and (11), the stress distribution along the wall of sleeve can be obtained by using Eq. (17). Substituting each correspondence value into Eq. (20), the distribution of the stress intensity factor of one single crack along the wall of sleeve is shown in Fig. 10. According to Landerman and Bamford (1984), the value of critical fracture toughness of 304 SS stainless steel is 265 ksi $\sqrt{\text{in.}}$ which is of course much larger than the stress intensity factor (K_{app}) of the crack calculated above. Therefore, unstable brittle fracture will never occur even the crack is finally a through-wall crack.

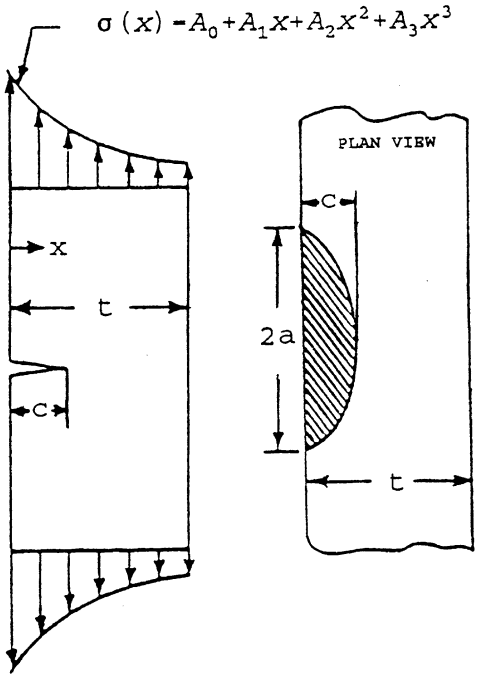

$$K_I = \sqrt{\frac{\pi c}{Q}}\,(G_0A_0 + G_1A_1c + G_2A_2c^2 + G_3A_3c^3),$$

Fig. 9. Stress distribution of a cylinder with a crack in radial direction.

5.2. Theoretical basis of crack growth

Fig. 11 shows a typical fatigue crack growth curve of steel. It is known that crack growth does not occur (non-propagating crack) if the stress intensity factor range ΔK_I is less than some threshold value ΔK_{th}. However, the crack will grow non-linearly within region I and linearly within II if ΔK_I is larger than ΔK_{th}. Region II is the main region to be concerned with during the fatigue fracture mechanics computation. Region III is usually neglected because it is a super-critical crack growth region (the growth rate of the crack is very high).

5.3. Stress intensity factor range

After substituting parameter values into Eq. (17) to find $\Delta\sigma_{th}$ and then approximating it by the polynomial form of Eq. (22), the stress intensity factor range (ΔK) under cyclic thermal stress loading can be obtained by using Eq. (20), i.e.,

$$\Delta K = \sqrt{\frac{\pi c}{Q}}(G_0A_0 + G_1A_1c + G_2A_2c^2 + G_3A_3c^3). \tag{23}$$

The solid line in Fig. 12 shows the distribution of stress intensity factor range of cyclic thermal stress due to thermal striping along the wall of the sleeve. It seems that there is no self-limiting effect of the secondary

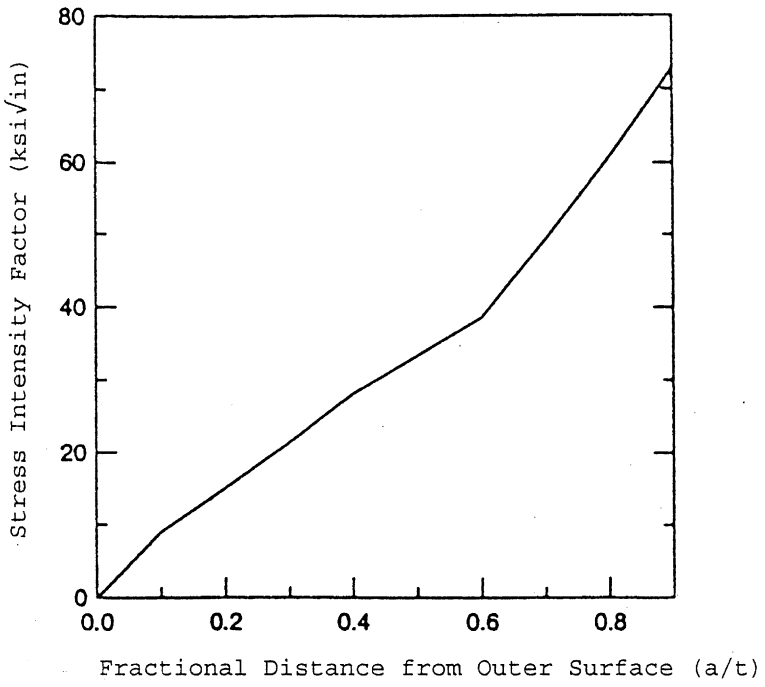

Fig. 10. Distribution of stress intensity factor of single crack along sleeve wall.

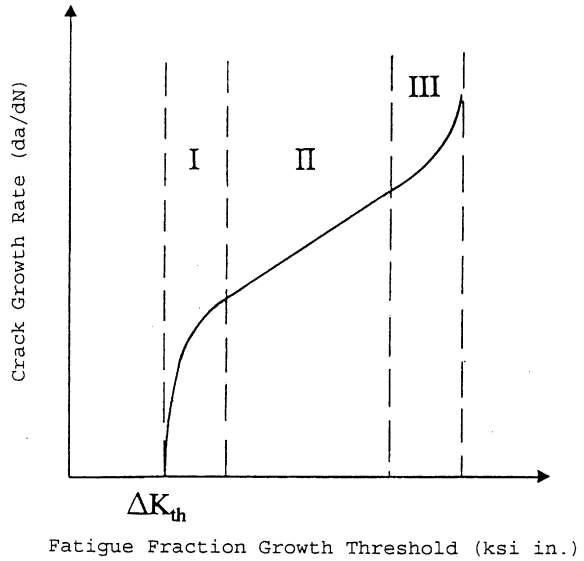

Fig. 11. Crack growth curve of steel.

stress, i.e., ΔK will increase monotonically with crack depth c. However, we still need to compare the fatigue fracture growth threshold (ΔK_{th}) to tell whether or not the high frequency fatigue growth will occur.

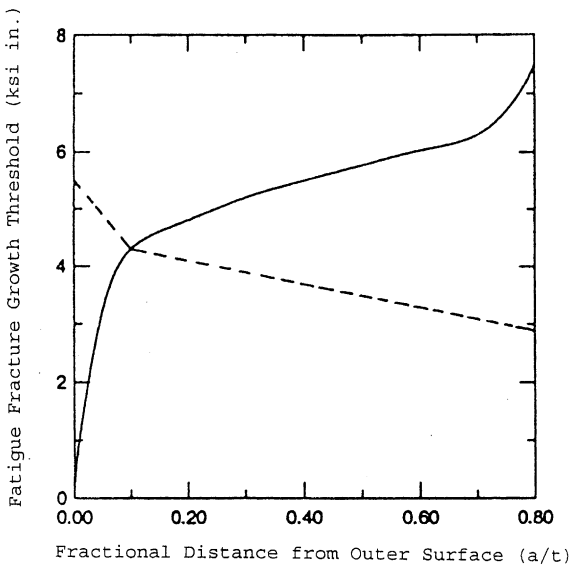

Fig. 12. Distributions of stress intensity factor range and fatigue fracture growth threshold along wall thickness.

5.4. Fatigue fracture growth threshold (ΔK_{th})

According to Barson (1976), the fatigue fracture growth threshold ΔK_{th} is a function of the ratio of stress intensity factors R and is independent of chemical components or mechanical properties for most materials. The experiment result shows the relationship between ΔK_{th} and R for austenitic steels, i.e.,

$$\Delta K_{\text{th}} = 6.4(1 - 0.85R) \quad \text{for} \quad R \geqslant 0.1 \tag{24}$$

$$\Delta K_{\text{th}} = 5.5 \quad \text{for} \quad R \leqslant 0.1,$$

where

$$R = \frac{K_{\min}}{K_{\max}} = \frac{\sigma_{\min}}{\sigma_{\max}}, \tag{25}$$

where $K_{\max}$, $K_{\min}$ are maximum, minimum stress intensity and $\sigma_{\max}$, $\sigma_{\min}$ are maximum, minimum applied normal stress, respectively.

Frost and Marsh (1974) also get the relationship between R and ΔK_{th} for austenitic stainless steel as in Table 1, where

Table 1
Fatigue fracture growth threshold for austenitic stainless steels

$R = K_{\min}/K_{\max}$	ΔK_{th} (ksi $\sqrt{\text{in.}}$)
0	5.5
0.33	5.4
0.62	4.2
0.74	3.7

$$K_{\min} = K\left(\sigma_{\mathrm{me}} - \frac{\Delta\sigma_{\mathrm{th}}}{2}\right), \tag{26}$$

$$K_{\max} = K\left(\sigma_{\mathrm{me}} + \frac{\Delta\sigma_{\mathrm{th}}}{2}\right), \tag{27}$$

where σ_{me} is the mechanical stress. The distribution of ΔK_{th} along the wall of the sleeve is clearly shown in Fig. 12 with the aid of Eqs. (3), (11), (17), (20), (25) and Table 1. ΔK_{th} curve decreases as R increases.

The intersection of solid line (ΔK_{app}, applied stress intensity factor range) and dash line (ΔK_{th}) in Fig. 12 is located at the point about 10% thickness from the outer surface of the wall. It means that the high frequency fatigue growth will occur after passing this point from the outer surface.

5.5. Lifetime estimation of sleeve

According to the analysis above, the crack will extend due to high frequency fatigue if the depth of the crack is larger than 10% of sleeve wall thickness. Based on the theory of fracture mechanics the unstable brittle fracture will not occur even though the crack through the wall. Therefore, there is no critical flaw size in this research. Although the through-wall crack will not cause any safety problem dramatically, it may still cause damage to the shaft for long term consideration. Hence, the thickness of the wall is the critical size to estimate the lifetime of sleeve.

For fatigue, the expression commonly used to relate the change in crack depth in Fig. 9 with the number of applied load cycles is known as the "Paris Law" by Paris and Erdogan (1963), i.e.,

$$\frac{\mathrm{d}c}{\mathrm{d}N} = C_m(\Delta K)^m, \tag{28}$$

where $C_m(1 \times 10^{-10})$ and m (3.176) are material constants for duplex stainless steel obtained by Landerman and Bamford [7]. Integration of Eq. (28) yields

$$N = \int \mathrm{d}N = \int_{c_{\mathrm{i}}}^{c_{\mathrm{f}}} \frac{\mathrm{d}c}{C_m(\Delta K)^m}. \tag{29}$$

Substitution of Eq. (20) into Eq. (29) leads to

$$N = \int_{c_{\mathrm{i}}}^{c_{\mathrm{f}}} \frac{\mathrm{d}c}{C_m\left[\sqrt{\frac{\pi c}{Q}}(G_0A_0 + G_1A_1c + G_2A_2c^2 + G_3A_3c^3)\right]^m}, \tag{30}$$

where $a_{\mathrm{i}} = 0.05$ in., $a_{\mathrm{f}} = 0.608$ in. (through-wall thickness). The lifetime of sleeve is therefore, 4.08×10^7 cycles (1.3 years) by using Runge–Kutta numerical method of Patel (1994) in Eq. (30).

6. Conclusions

A network of cracks has been found on the surface of a sleeve a of reactor coolant pump at a nuclear power plant due to thermal striping phenomenon. As already noted, the average circumferential stress along the wall of sleeve is 20 ksi. The correspondence value of stress intensity factor K_{I} is much smaller than critical fracture toughness K_{Ic}. Consequently, unstable brittle fracture will never occur even though the crack finally through the wall.

On the other hand, even only 0.2 in. (1/3rd wall thickness) from outer surface of sleeve will be affected by temperature fluctuation the high frequency fatigue model will, however, occur after the crack depth is larger than 10% of the wall thickness.

To estimate more conservative, the through-wall time (1.3 years) for a single crack is assumed to be the lifetime of sleeve.

Acknowledgements

This work was sponsored by National Science Council, Republic of China, through Grant NSC 88-2212-E-216-003 at Chung-Hua University is greatly acknowledged.

References

ASME, 1989. Boiler and Pressure Vessel Code, Section III.

Barson, J.M., 1976. Fatigue behavior of pressure vessel steel. Int. J. Pressure Vessels Piping 1, 206–213.

Frost, N.E., Marsh, K.J., 1974. Metal Fatigue. Oxford University Press, London.

Gruter, L., Huget, W., 1982. Fatigue crack behavior under thermal stress. Int. J. Pressure Vessels Piping 10, 355–359.

Jiang, Z.D., Petit, J., Bezine, G., 1991. Stress intensity factors of two parallel 3D surface cracks. J. Engng. Fract. Mech. 40, 345–354.

Landerman, E.I., Bamford, W.H., 1984. Fracture toughness and fatigue characteristics of centrifugally cast stainless steel pipe after simulated service conditions. Westinghouse Electric Corporation, Pittsburgh.

Paris, P.C., Erdogan, F., 1963. Critical analysis of crack propagation laws. Trans. ASME J. Basic Engng. D 85, 528–534.

Patel, V.A., 1994. Numerical Analysis. Saunders College Publishing, New York.

Raju, I.S., Newman, J.C., 1982. Stress intensity factors for internal and external surface cracks in cylindrical vessels. J. Pressure Vessel Tech. 104, 293–298.

Sun, B., Kim, J., Lin, C.L., Sursock, J.P., 1982. Baseline programs for application to pressurized thermal shock. EPRI Thermal-Hydraulic Research.

Tada, H., Paris, P.C., Irwin, G.R., 1985. The Stress Analysis of Cracks Handbook. Paris Productions Inc., St. Louis.

Timoshenko, S.P., Goodier, J.N., 1970. Theory of Elasticity. McGraw-Hill, New York.